In-situ photopolymerization of oriented liquid-crystalline acrylates, 5[a)]

Influence of the alkylene spacer on the properties of the mesogenic monomers and the formation and properties of oriented polymer networks

Dirk J. Broer, Grietje N. Mol*

Philips Research Laboratories, P. O. Box 80.000, 5600 JA Eindhoven, The Netherlands

Ger Challa

State University of Groningen, Laboratory of Polymer Chemistry, Nijenborgh 16, 9747 AG Groningen, The Netherlands

(Date of receipt: April 6, 1990)

SUMMARY:

The photoinitiated bulk polymerization of macroscopically oriented 1,4-phenylene bis{4-(ω-acryloyloxyalkyloxy)benzoate} produces densely crosslinked oriented polymer networks. The influence of the length of the alkylene spacer between the aromatic central core and the polymerizable acrylate end-groups on the mesomorphic behaviour of the monomer, the molecular orientation in the monomeric and polymeric state and the process of photoinitiated polymerization in the ordered state is studied. Some optical properties of the oriented networks are presented.

Introduction

In previous investigations we demonstrated that the photoinitiated bulk polymerization of liquid-crystalline (LC) diacrylates in their oriented state leads to densely crosslinked oriented polymer networks[1,2]. Macroscopic orientation of the low-viscous nematic monomers is achieved on a substrate coated with a unidirectionally rubbed thin polymer film, e. g., polyimide. Subsequently, the monomeric alignment is permanently fixed by the fast photoinitiated chain crosslinking of the diacrylates. Both coatings and free-standing films, exhibiting highly anisotropic optical and mechanical properties, have been produced.

The monomers studied were 1,4-phenylene bis{4-(6-acryloyloxyhexyloxy)benzoate} (Tab. 1, compound **6h**) and its analog with a methyl substituent in the central ring (**6m**). In both monomers the polymerizable acrylate end-groups are separated from the rod-like aromatic core by a hexamethylene spacer group. Comparable spacers are incorporated between the mesogenic unit and the polymer chain of LC side-chain polymers, and their function is to provide enough rotational freedom to allow molecular alignment in the polymeric phase by mechanically decoupling the mesogenic unit from the

[a)] Part 4, cf.[2].

 CCC 0025-116X/91/$03.00

polymer main chain[3,4]. In our case, however, the mesogenic units are already ordered in the monomeric phase and the spacer is meant to allow the formation of polyacrylate chains independently from the topology of the mesogens. Consequently, for photo-initiated polymerizable diacrylates, the length of the alkylene spacer may have a significant influence on the polymerization kinetics and on the ordering properties of the polymer networks which will be discussed in this paper.

As the oriented polymer networks are promising materials for optical applications, special attention is paid to the optical properties of these materials. The mechanical properties[5] and the anisotropic thermal expansion[6] of oriented networks will be discussed in forthcoming publications.

Experimental part

Materials

A general route for the synthesis of the liquid-crystalline diacrylates was presented in an earlier publication[1]. Monomers, **4h**, **5h**, **6h**, **11h**, **4m**, **5m** and **6m** (Tab. 1) were synthesized at the Philips Research Laboratories, while **8h** and **10h** were synthesized at Syncom B. V., Groningen, The Netherlands. For photopolymerization, mixtures were made with 1 wt.-% α,α-dimethoxydeoxybenzoin (Ciba Geigy, Basle, Switzerland) and 100 ppm *p*-methoxyphenol (Fluka A. G., Buchs, Switzerland). For the UV-VIS dichroic measurements, 0,5 wt.-% of a yellow dichroic bis-azo dye (SI-486, Mitsui Toatsu Dyes, Ltd., Tokyo, Japan) was added to the monomer formulations.

Experimental techniques

Experimental methods for the determination of transition data and photopolymerization rate by DSC, macroscopic orientation of the monomers, photopolymerization and measurement of refractive indices have been described in earlier publications[1,2,7,8]. The birefringence Δn as a function of wavelength is measured by recording UV-VIS spectra (Philips PU8740) of 5 μm films between crossed polarizers[9]. Thicknesses of monomer and polymer films are determined interferometrically.

Dichroic measurements in the UV-VIS region were performed in glass cells provided with rubbed polyimide and temperature-controlled by a hot stage (Mettler FP82/FP80). Dichroic effects from the illumination source and the director are accounted for by using depolarizers. The reference baseline was recorded with oriented monomer or polymer without dye.

Dichroic infrared measurements were performed by means of a Nicolet 7000 FTIR spectrophotometer provided with a CaF_2/Al grid polarizer with an efficiency of 98% at the wavelengths studied. Free-standing films of 5 μm thickness were aligned under a polarizing microscope parallel to the IR polarizer and measured in the spectrophotometer at 0° and at 90°.

Order parameters and molecular conformation

The order parameter $\langle P_2 \rangle$ describes the average value of the second order Legendre polynominal $(3\cos^2\phi - 1)/2$, where ϕ is the angle between the molecular long axis and the director. We have provided $\langle P_2 \rangle$ with the subscripts *n*, *G* and *i*, indicating the method of determination from refractive indices, guest-dye UV-VIS dichroism and IR dichroism, respectively. Assuming an isotropic internal field[10,11], $\langle P_2 \rangle_n$ was calculated from the ordinary refractive index n_0 and the extraordinary refractive index n_e, using the equation $\langle P_2 \rangle_n = (\bar{\alpha}/\Delta\alpha)(n_e^2 - n_0^2)/(\bar{n}^2 - 1)$, in which $\Delta\alpha$ is the difference between the electronic molecular polarizability parallel and perpendicular to the molecular axis, $\bar{\alpha}$ the mean polarizability and $\bar{n}$ the mean refractive index. The applied polarizability term $\Delta\alpha/\bar{\alpha}$, as estimated according to the Haller method[12,13], is 0,55, 0,54, 0,52, 0,51 and 0,50 for **4h**, **5h**, **6h**, **8h** and **10h**, respectively, and 0,55, 0,51 and 0,52 for **4m**, **5m**, **6m**.

The order parameter of the dichroic bis-azo dye probe is calculated[14,15] from $\langle P_2 \rangle_G = (A_\parallel - A_\perp)/(A_\parallel + 2A_\perp)$, where $A_\parallel$ and $A_\perp$ are the absorbances of the local absorption maximum at 406 nm parallel and perpendicular to the orientation direction, respectively. At higher temperatures the absorption maximum shifts to somewhat shorter wavelengths. The transition moment of the dye is assumed to be parallel to its long molecular axis.

The order parameter of the individual moieties was determined by IR dichroism[16,17], using the equation $\langle P_2 \rangle_i = (A_\parallel - A_\perp)/(A_\parallel + 2A_\perp)$, where $A_\parallel$ and $A_\perp$ are the absorbances of the IR bands, corrected for the polarizer efficiency[18]. Local field corrections have been neglected. The introduction of a correction for an isotropic local field according to Vuks[10] would increase the positive infrared order parameters by about 5%, based on the ratio of n_0 and n_e estimated from polarized interference in the IR spectrum.

For the calculation of the molecular conformation, MNP2 software[19,20], as a part of the CHEMX molecular modelling program[21], was used. The minimized energy calculations refer to isolated molecules ignoring dispersive interactions in the liquid-crystalline state.

Results and discussion

Mesomorphism of the monomers

The monomers studied and their LC transition temperatures are summarized in Tab. 1. All monomers show polymorphism in the crystalline (K) state, and the melting temperatures (T_m) presented correspond to the highest values observed. The monomers melt at higher temperatures, with a small tendency of T_m to decrease with increasing spacer length.

Above T_m the R = H homologues with $x \leq 6$ directly become nematic, while for x = 8 to 11 the formation of a smectic-C (S_C) phase is observed first. During supercooling of these samples, often higher order smectic phases are observed which

Tab. 1. The LC monomers studied and their transition temperatures. The general chemical formula of the monomers is:

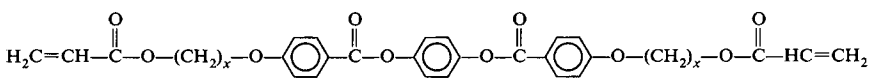

Monomer	x	R	Transition temp. in °C[a]						
4h	4	H	K	107	S	—	N	165	I
5h	5	H	K	92	S	—	N	170	I
6h	6	H	K	108	S	(88)	N	155	I
8h	8	H	K	82	S	108	N	148	I
10h	10	H	K	87	S	112	N	137	I
11h	11	H	K	81[b]	S	114	N	134	I
4m	4	CH_3	K	80	S	—	N	120	I
5m	5	CH_3	K	93	S	—	N	124	I
6m	6	CH_3	K	86	S	—	N	116	I

[a] K: crystalline, S: smectic, N: nematic, I: isotropic.
[b] Smectic transitions are observed at 87 and 95 °C.

were not further characterized. For $x = 6$, a monotropic S_c phase is formed during supercooling.

The clearing temperature (T_c) at the transition nematic (N) to isotropic (I) decreases with increasing spacer length. A small odd-even effect, with the highest T_c for the two $x = 5$ spacered samples, can be observed. Substitution of a methyl group in the central ring suppresses the transition temperatures as well as the tendency to form smectic phases. These observations are in accordance with observations on phenylene bis(alkoxybenzoates)[22].

The thermodynamic parameters of the thermal transitions are summarized in Tab. 2. The enthalpy and entropy of the N → I transition both increase with spacer length and the odd-spacered samples exhibit relatively high values. Introducing the CH_3 group in the central ring increases both the transition enthalpy and entropy, due to interlocking of the substituent reducing the longitudinal motions[23]. The tendencies are in accordance with the behaviour found for conventional liquid crystals[24].

Tab. 2. Transition enthalpy and entropy of the various monomers

Monomer	Enthalpy in kJ/mol							Entropy in J/(mol · K)						
4h	K	57	S	—	N	0,8	I	K	150	S	—	N	1,9	I
5h	K	54	S	—	N	1,3	I	K	148	S	—	N	2,9	I
6h	K	67	S	(0,6)	N	0,9	I	K	176	S	(1,7)	N	2,2	I
8h	K	40	S	0,8	N	1,4	I	K	113	S	2,0	N	3,2	I
10h	K	49	S	0,7	N	1,4	I	K	136	S	1,8	N	3,5	I
11h	K	67	S	0,5	N	1,7	I	K	189	S	1,3	N	4,2	I
4m	K	68	S	—	N	1,4	I	K	194	S	—	N	3,6	I
5m	K	60	S	—	N	1,9	I	K	164	S	—	N	4,7	I
6m	K	61	S	—	N	1,6	I	K	170	S	—	N	4,1	I

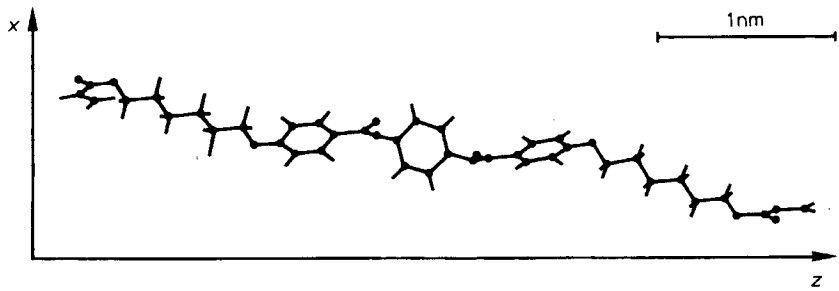

Fig. 1. Calculated minimized energy conformation of monomer **6h**

Monomer conformation

Fig. 1 shows the calculated minimized-energy conformation of **6h**. Displayed is the most extended mesogenic unit conformation with a centre of symmetry in the central

ring. The two outer phenyl rings are twisted with respect to the central ring, and their *para*-axes make an angle of 24°. The calculated twist angles correspond to crystallographic data of phenyl benzoate[25]. Torsion over one of the aromatic ester linkages yields a mirror-symmetric conformation with a virtually identical heat of formation as the displayed one.

The torsion angle between the plane of the C—C bonds in the spacer and the plane of the outer ring at the Ph—O—C bonds is ±90°. X-ray measurements in the S_c phase of **6h** showed a periodicity conformal to the extended molecular length, pointing to a favourable all-*trans* conformation of the spacer[26]. However, shape transformations by *trans-gauche* excitation are known to have rather low activation energies[27].

The plane of the acrylate group, comprising its three carbon and two oxygen atoms, lies perpendicular to the plane of the spacer. Two favourable conformations are calculated: an extended conformation which is shown at the right-hand side of Fig. 1 and the left-hand side conformation in which the acrylate group is folded back. The spacer length affects the position of the acrylate group which can cause the odd-even effect in the mesogenic transition data.

Degree of orientation of the monomer before polymerization

The order parameter $\langle P_2 \rangle$ of the macroscopically oriented monomers is determined from refractive index measurements and from UV-VIS dichroism of a bis-azo dye guest. The lower curve in Fig. 2 is the order parameter obtained from the refractive indices, $\langle P_2 \rangle_n$, of the various monomers studied as a function of the reduced temperature $T(\mathrm{K})/T_c(\mathrm{K})$. Within the experimental error all data fall on one curve, according to Maier-Saupe's mean-field theory[28], which can be fitted[29] by $\langle P_2 \rangle = (1 - aT/T_c)^b$ with $a = 0{,}98$ and $b = 0{,}22$.

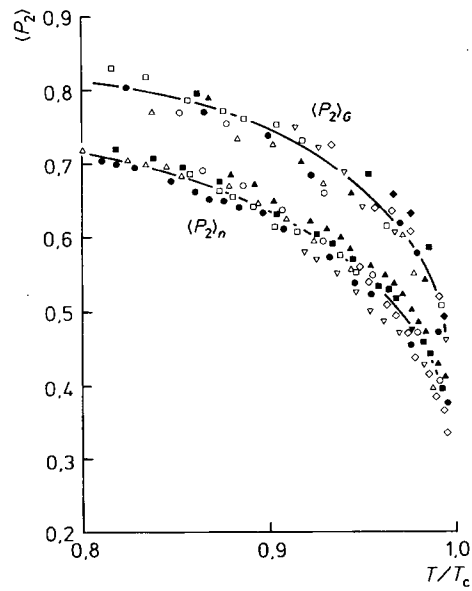

Fig. 2. The order parameter as derived from refractive indices $\langle P_2 \rangle_n$ and from UV-VIS dichroic measurements of a dichroic probe $\langle P_2 \rangle_G$ vs. reduced temperature T/T_c. (□): **4h**; (△): **5h**; (○): **6h**; (▽): **8h**; (◇): **10h**; (◆): **11h**; (■): **4m**; (▲): **5m**; (●) **6m**

In order to establish a high degree of orientational order with $\langle P_2 \rangle_n \rightarrow 0{,}7$, a broad temperature range of the monomeric N-phase is required. For larger spacer lengths, $\langle P_2 \rangle_n$ in the nematic phase reaches no more than 0,6 because of the occurrence of the S_c phase. Macroscopic ordering in this phase is limited due to the feather-like domain structure as observed by polarizing microscopy.

Fig. 2 shows that the guest order parameter $\langle P_2 \rangle_G$ is higher than $\langle P_2 \rangle_n$. This is a common phenomenon for well-dissolving dye guests[30,31] with a transition moment parallel to their long axis. The absence of conformational changes of flexible end-groups in the dye molecules narrows their distribution function with respect to that of the mesogenic diacrylates. In general, $\langle P_2 \rangle_G$ can be considered as a measure of the distribution function of the stiff aromatic parts of the molecules, whereas $\langle P_2 \rangle_n$ represents the whole molecule, still with an emphasis on the aromatic part due to polarizability differences between aromatic and aliphatic moieties. The presence of the acrylate group enhances the contribution of the end-groups to $\langle P_2 \rangle_n$ when compared to conventional liquid crystals containing less polarizable alkyl or alkoxy end-groups.

Polymerization in the nematic phase

Photoinitiated polymerization of the monomers in their oriented nematic state results in all cases in homogeneously oriented polymeric films. As observed under a polarizing microscope, the initial monodomain-like texture of the monomer is maintained during polymerization. There is only a colour change due to a slight change in the optical retardation defined by the product of the thickness d and the birefringence Δn. The thickness decreases due to polymerization shrinkage[32,33], while Δn can either increase or decrease depending on the polymerization temperature or the presence of the methyl substituent.

Fig. 3 shows the polymerization rate R_p versus conversion for **5h** irradiated with a fluorescent lamp emitting 350 nm light with an intensity of 0,2 mW · cm^{-2}. The shape of the curves in this figure is exemplary for all the monomers studied. At low conversions the rate increases due to autoacceleration by suppression of the termination reaction because of a limited diffusion of the reactive end-group of a polymerizing chain in a network[34,35]. The maximum rate $(R_p)_{max}$ is reached at 20–25% conversion. At higher conversions the rate decreases due to monomer depletion and even more due to a limited diffusional mobility of the remaining acrylate groups. At 70–80% conversion the rate virtually becomes zero when measured by DSC. IR analysis revealed that from this point the reaction may still proceed at a low rate to a complete disappearance of the vinyl absorption bands at 1 636 and 840 cm^{-1} for all monomers after 15 min irradiation.

The polymerization temperature T_p has only a marginal influence on the shape of the polymerization curves (see Fig. 3) but a large effect on the rate itself. Fig. 4 shows $(R_p)_{max}$ as a function of T_p for the various monomers. In the nematic temperature region all monomers polymerize very fast, with rates comparable to those of isotropic diacrylates[35]. At higher temperatures the propagation-depropagation equilibrium suppresses the rate which approaches zero above 200 °C (ceiling temperature).

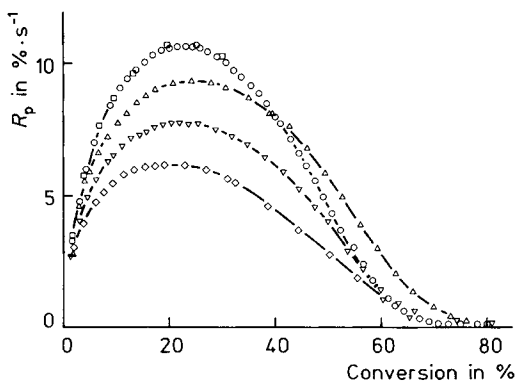

Fig. 3. Polymerization rate of **5h** (in % C=C reacted per second) as a function of the conversion (% C=C bonds reacted, calculated with respect to the initial concentration) at various polymerization temperatures; (□): 90 °C; (○): 110 °C; (△): 130 °C; (▽): 150 °C; (◇): 170 °C

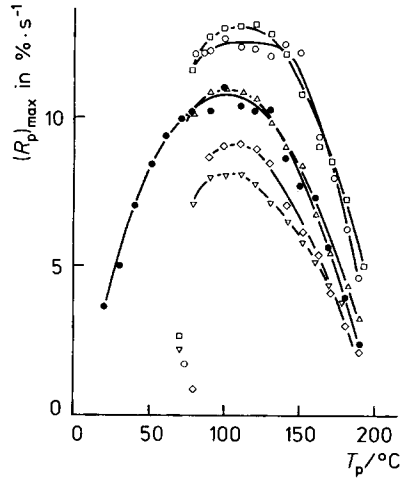

Fig. 4. Maximum polymerization rate $(R_p)_{max}$ as a function of polymerization temperature T_p. The same symbols are used as in Fig. 2

In the case of conventional isotropic diacrylates[35] chain transfer via abstraction of the α-H of the acrylate enhances termination and therefore suppresses the autoacceleration above 90 °C. For the nematic diacrylates, however, the rate maximum is observed at somewhat higher temperatures (Fig. 4), indicating that chain transfer is less predominant in ordered systems.

Below 80 °C most samples crystallize and low polymerization rates are measured, as shown in Fig. 4 by the isolated low-rate data points around 70 °C. Only the methyl-substituted samples allow polymerization in the nematic LC phase down to temperatures as low as room temperature in a largely supercooled state. In that case the overall polymerization rate is low not primarily by a decreased monomer reactivity but rather due to a limited diffusional mobility caused by a high initial viscosity and by vitrification when the glass transition is passed during polymerization.

Polymerization in the smectic phase

The monomers **8h** and **10h** exhibit a stable S_c and **6b** a monotropic S_c phase. As mentioned above, the surface-induced orientation of the monomers in this phase revealed a macroscopic ordering with local director fluctuations resulting in the feather-like texture. Polymerization of these monomers in their oriented S_c phase fixes this texture. Fig. 5 shows the photographs of a polymer film with a frozen-in S_c texture between crossed polarizers (a) with the front polarizer at 45° and (b) parallel to the rubbing direction on both substrates between which the polymer film was produced. The transmissive parts in Fig. 5 (b) can be successively extinguished by rotation of the samples, which illustrates the presence of director fluctuations.

There is no remarkable difference in the overall kinetics of polymerization between the smectic and the nematic phases. Changes observed in Fig. 4 near the transition are of the same order as those caused by temperature variations in the absence of a transition.

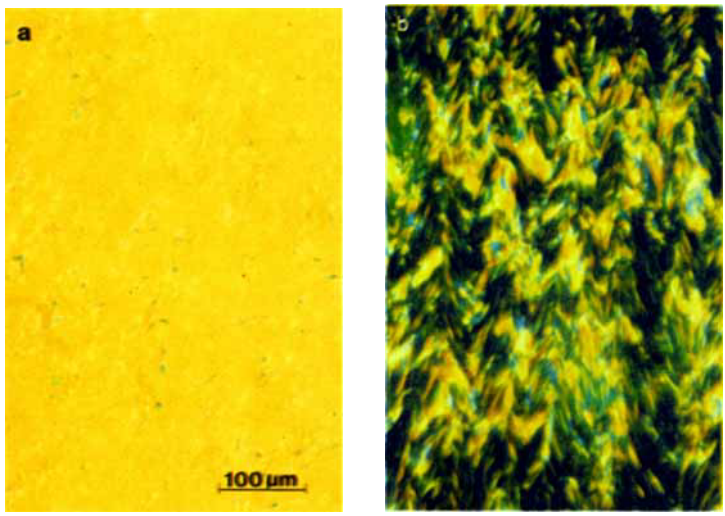

Fig. 5. Polarization microscope photographs of a frozen-in smectic phase of poly(**8h**) with the director at an angle of 45° (a) and 0° (b), resp.

Polymerization near phase transitions

Polymerization in the nematic monomer phase within a few degrees above the smectic transition temperature results in opaque films. This effect becomes more pronounced when the UV light intensity is reduced. From linear LC side-chain polymers it is known[3,4,36] that the polymers exhibit higher LC transition temperatures than their corresponding monomers and polymerization of bulk LC monoacrylate raises the S → N transition by several tens of degrees[7,8]. Polymerization of the

nematic diacrylate fixes the nematic texture. However, near its transition to smectic, director fluctuations are introduced when this transition is (locally) passed at increasing molecular weight. Light scattering is then caused by the resulting refractive index fluctuations.

A similar observation is made when the polymerization is carried out in the isotropic state just above T_c. In that case the initially clear films become turbid due to a (local) transition to the nematic phase. At higher temperatures continuously clear films are produced again.

For polymerizations performed just below a transition, the temperature increase originating from the heat of polymerization under high-intensity irradiation might cause a phase transition. This did not occur under the conditions used.

Degree of orientation of the oriented polymer networks

We compared the order parameters of the oriented networks with those of the monomers by refractive index and dichroic measurements. Analysis of the refractive indices provides information on the overall molecular orientation of the network, with emphasis on the aromatic mesogenic moieties forming the crosslinks between the poly(acrylate) main chains. For the calculation of $\langle P_2 \rangle_n$ of the polymers, the monomeric $\Delta a/\bar{a}$ values are used. Extrapolation methods to $\langle P_2 \rangle \rightarrow 1$ at zero temperature for a more appropriate determination of $\Delta a/\bar{a}$ cannot be applied because the formation of a perfectly ordered structure is hampered by the network.

Fig. 6 shows both the $\langle P_2 \rangle_n$ and the $\langle P_2 \rangle_G$ data of the polymers. The $\langle P_2 \rangle_n$ data concern networks obtained by photopolymerization of the various monomers at an equal initial monomeric order parameter $\langle P_2 \rangle_n = 0{,}59$. The influence of the spacer length on the degree of orientation of the networks is relatively small, with somewhat

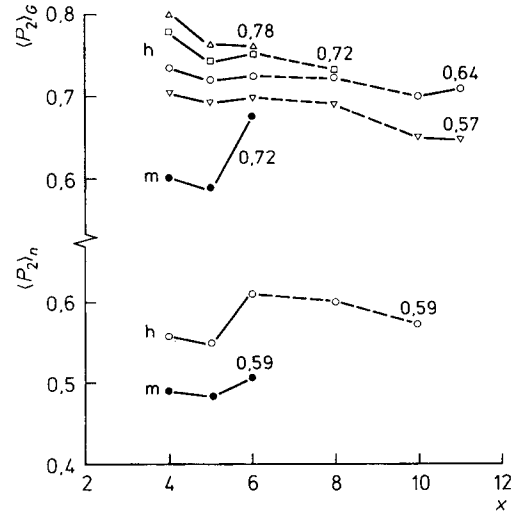

Fig. 6. Order parameter obtained from refractive indices $\langle P_2 \rangle_n$ and from UV-VIS dichroism $\langle P_2 \rangle_G$ of oriented polymer networks as a function of spacer length x. The numbers indicate the corresponding initial order parameters in the monomeric state, h and m refer to hydrogen or methyl substituent in the central ring, resp.

lower values at $x < 6$. The $\langle P_2 \rangle_n$ of the methyl-substituted polymers is considerably lower than that of the non-substituted samples.

The $\langle P_2 \rangle_G$ of the non-polymerizable dye guest in the polymer networks are shown in the upper part of Fig. 6. The various curves are obtained by polymerization at different temperatures such that the initial $\langle P_2 \rangle_G$ of the monomers are as indicated. In general, high guest order parameters, $\langle P_2 \rangle_G$, are measured for the various polymers corresponding to the analogous measurements in the monomeric phase. The influence of the spacer length on $\langle P_2 \rangle_G$ of the oriented networks is small, with a slight tendency of $\langle P_2 \rangle_G$ to decrease with increasing spacer length. The effect of a somewhat lower ordering in the case of the smaller spacer lengths, as calculated from the refractive indices, is not observed here for the non-substituted samples.

The influence of the initial monomeric order parameter (i.e., the polymerization temperature) on the degree of orientation of the polymer network is the same for non-substituted monomers. At low initial monomeric ordering, e.g., $\langle P_2 \rangle_G = 0{,}57$, the orientation increases during polymerization, whereas at an initial monomeric ordering as high as $\langle P_2 \rangle_G = 0{,}78$, the orientation remains the same within the experimental error or decreases slightly. The presence of the methyl group decreases $\langle P_2 \rangle_G$, in agreement with the results obtained from the refractive index measurements.

Infrared dichroic measurements were carried out in order to compare the degree of orientation of the mesogenic moieties with that of the flexible spacers. Tab. 3 summarizes the various absorption bands studied, and Tab. 4 presents the $\langle P_2 \rangle_i$ of the individual moieties calculated from their dichroic ratios without any correction for the direction of the transition moment in the molecular frame. The order parameter of the phenylene groups, measured from the ring breathing modes at 1 510 and 1 608 cm^{-1}, lie between 0,48 and 0,70, depending on monomer type and polymerization temperature. There is such a remarkable difference between $\langle P_2 \rangle_{1\,608}$ and $\langle P_2 \rangle_{1\,510}$ that

Tab. 3. Absorption bands studied by polarized FTIR and the angle γ between the vector of the transition moment and the molecular z-axis

Frequency in cm^{-1}	Assignment	Moiety	γ
2 938	$\nu_s(CH_2)$	Sym. str. spacer/main chain	82°
1 608	ν(C=C)	Symm. skelet. vibr. benzene ring	8°
1 510	ν(C=C)	Asymm. skelet. vibr. benzene ring	16°
848	δ(CH)	Arom. CH out-of-plane vibr.	79° [a]
762	δ(CH)	*ibid.*	79° [a]

[a] The γ values presented are the average over the three benzene rings.

they cannot be attributed to the same vibration of the same moiety. An explanation is that the IR absorption band at 1 608 cm^{-1} is dominated by the symmetric skelet vibration of benzenes asymmetrically *para*-substituted by an electron donor and an electron acceptor, respectively[37]. This means that the outer rings contribute more to the

Tab. 4. Order parameters $\langle P_2 \rangle_i$ of various moieties obtained from dichroic infrared measurements at the indicated frequencies and the calculated molecular biaxiality D

Sample	T_p/T_c	$\langle P_2 \rangle_i$					D
		frequency in cm^{-1}					
		2 938	1 608	1 510	848	762	
Poly(**4h**)	0,96	−0,16	0,56	0,48	−0,29	−0,32	0,05
Poly(**5h**)	0,96	−0,15	0,61	0,60	−0,31	−0,31	0,01
Poly(**6h**)	0,86	−0,17	0,69	0,65	−0,36	−0,37	0,04
Poly(**6h**)	0,92	−0,18	0,68	0,62	−0,33	−0,35	0,00
Poly(**6h**)	0,96	−0,19	0,66	0,60	−0,36	−0,33	0,03
Poly(**6m**)	0,96	−0,15	0,56	0,51	−0,28	−0,31	0,03
Poly(**8h**)	0,96	−0,21	0,63	0,59	−0,33	−0,36	0,05
Poly(**10h**)	0,96	−0,22	0,65	0,60	−0,36	−0,36	0,04

intensity of this band than the inner ring. The opposite occurs at the 1 510 cm^{-1} band, whose asymmetic vibration gives the highest absorption for benzenes which are symmetrically *para*-substituted, i. e., for the central ring. The higher value of $\langle P_2 \rangle_{1\,608}$ in comparison with $\langle P_2 \rangle_{1\,510}$ now leads to the conclusion that the *para*-axis of the outer rings lies more parallel to the long molecular axes than the *para*-axis of the central ring.

The order parameter $\langle P_2 \rangle_z$ of the long molecular axis of the aromatic core (z-axis, see Fig. 1) can be calculated from $\langle P_2 \rangle_z = \langle P_2 \rangle_i / P_2(\gamma)$, where $P_2(\gamma) = (3\cos^2\gamma - 1)/2$ is a constant determined by the angle γ between the transition dipole moment and the molecular z-axis. For the most convenient choice of the z-axis, namely, along the line between the two ether oxygens at both ends of the aromatic core in its extended conformation, the values of γ are summarized in Tab. 3. So, by introducing an angle of 8° for the band at 1 608 cm^{-1} dominated by the outer rings and one of 16° for the band at 1 510 cm^{-1} dominated by the inner ring, Fig. 7 shows that the resulting order parameters of the z-axis become very similar.

The aromatic C—H absorption bands at 848 and 762 cm^{-1} are out-of plane vibrations perpendicular to the rings and consequently yield negative order parameters, as presented in Tab. 4. In the case of a cylindrical symmetry of the molecules, they should correspond to $\langle P \rangle_i$ of the benzene skeletal vibrations when multiplied by a factor of −2. The lower multiplication factor indicates the existence of molecular biaxiality, which can be quantified by an order parameter D defined by $D = \langle P_2 \rangle_x - \langle P_2 \rangle_y$, where the subscripts x and y refer to the two molecular coordinates perpendicular to the z-axis. The values of D, calculated according to Kiefer and Baur[17], are presented in the last column of Tab. 4.

They show that the biaxiality of the mesogenic units in the networks is in between those found for low-molecular-weight two-ring mesogens based on biphenyl and phenyl benzoate, respectively. This observation supports the molecular conformation presented in Fig. 1 consisting of two nearly parallel outer rings and a central one with a considerable twist.

From the $\langle P_2 \rangle_{2\,938}$ of Tab. 4 the mean orientation of the aliphatic CH_2 groups in the spacer and the polymer main chain can be deduced. The negative sign indicates that

the direction of the transition moment of the C—H stretch vibration is preferentially perpendicular to the director. In order to gain an impression of the degree of orientation of the spacer groups, the data of Tab. 4 are corrected for the angle γ of the average transition moment with the molecular z-axis and for a non-dichroic background caused by the CH_2 group in the acrylate main chain. Arbitrary, no preferential ordering was assumed in the main chain. Fig. 7 illustrates that the resulting order parameter of the spacer is lower than that of the aromatic core and decreases further for smaller spacer lengths. The low $\langle P_2 \rangle_z$ of the $x = 5$ spacer indicates that the topology of an odd-spacered acrylate end-group in the monomer forces the spacer to change its extended conformation during polymerization.

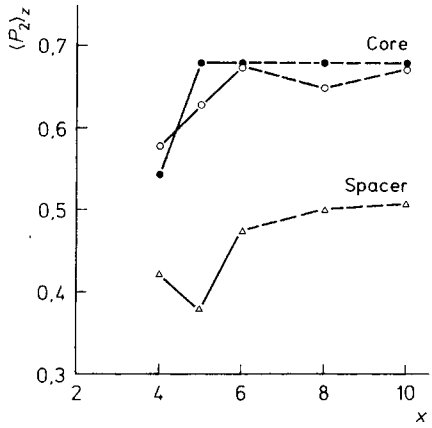

Fig. 7. Order parameter of the long molecular axis, $\langle P_2 \rangle_z$, calculated from the infrared dichroic data of various absorption bands vs. spacer length x. (○): 1608 cm^{-1}; (●): 1510 cm^{-1}; (△): 2938 cm^{-1}. All samples were polymerized at a reduced temperature $T/T_c = 0{,}96$

A comparison of the results of the various techniques shows that the $\langle P_2 \rangle_G$ values of the polymers with $x \geq 6$ are of the same order as the $\langle P_2 \rangle_z$ values of the aromatic core, when polymerized at equal reduced temperatures. As expected, the $\langle P_2 \rangle_n$ values lie in between the $\langle P_2 \rangle_z$ of the aromatic core and of the alkylene spacer, respectively.

A remarkable difference is found at $x < 6$ between the refractive index and the dichroic IR measurements, which both reveal relatively low order parameters, and the dichroic ratio of the dye which shows high order parameters. As an explanation, the decrease of the order parameter at small spacer lengths is proposed to be mainly attributable to the constrained arrangement of the mesogens, imposed by the acrylate main chains. This leads to conformational changes within the structure of the mesogenic unit, e. g., a torsion over the aromatic ester groups with increased values for the angle γ, but does not change the order parameter of the long axes as such which is represented by the guest order parameter.

The presence of a methyl group in the central ring hinders the torsional rotation over the aromatic ester linkages, which leads to a decrease of the order parameter of the molecular rods as a whole.

Optical properties

Coatings and films of the investigated diacrylates are transparent to visible light without noticeable light scattering in films with a thickness ≤ 60 µm. In the UV region the polymer network itself starts to absorb below 325 nm. The photoinitiator has an absorption maximum at 335 nm without any dichroism. The optical properties in the 300 to 400 nm region therefore largely depend on the type of photoinitiator, its concentration, its decay by UV irradiation and its yellowing by photodegradation.

Fig. 8 shows two examples of a transmission spectrum of a polymer film between crossed polarizers. Their shape is characteristic for uniaxial films. The transmission minimum around 700 nm corresponds to the first-order extinction ($d\Delta n/\lambda = 1$), while the sequence of following minima corresponds to the higher order extinctions. The resulting birefringence Δn as a function of the wavelength λ, shown in Fig. 9, is caused by a larger dispersion for n_e than for n_0.

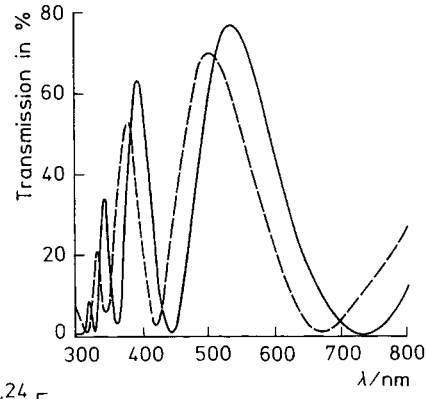

Fig. 8. Transmission of a 5,1 µm film of poly(**4h**) (solid line) and a 5,5 µm film of poly(**10h**) (dashed line) between crossed polarizers with the director at 45°

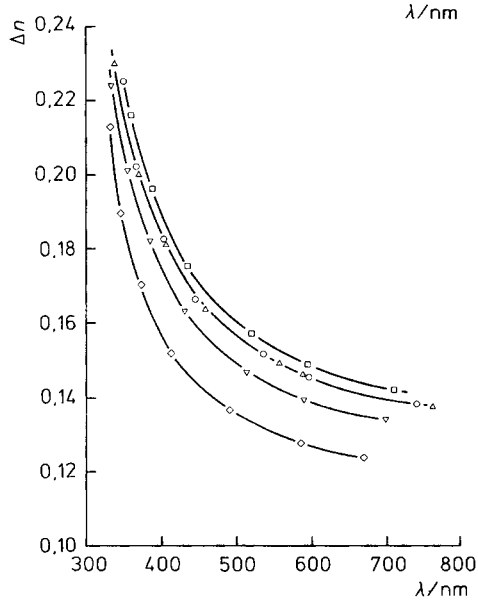

Fig. 9. Dispersion of the birefringence of the polymer networks indicated by the same symbols as in Fig. 2

The principal refractive indices at 589 nm are shown in Fig. 10 for the various polymers, all polymerized at T_p/T_c = 0,93. The decrease in both n_e and n_0 with increasing spacer length must be mainly assigned to the decrease in aromaticity of the molecules. The methyl-substituted homologues are less ordered and therefore have a lower n_e and a higher n_0. The refractive indices can be varied by selecting other polymerization temperatures, thus creating polymers with a different degree of orientation. As a consequence, any n_e between 1,64 and 1,70 can be tailor made. The variation in n_0 is less pronounced, i.e., from 1,52 to 1,55.

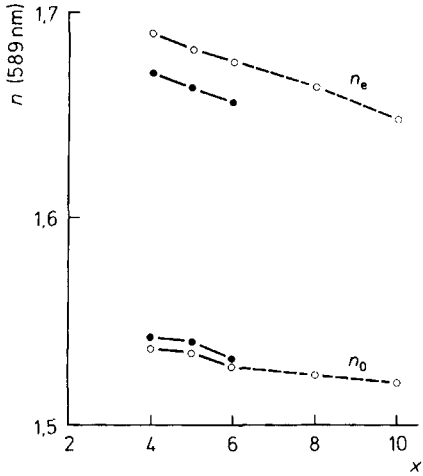

Fig. 10. Ordinary (n_0) and extraordinary refractive index (n_e) as a function of spacer length of the non-substituted (○) and the methyl-substituted polymers (●). All polymer networks were polymerized at T_p/T_c = 0,93

The temperature dependence of Δn as determined from the optical retardation is shown in Fig. 11. In general, the oriented polymer networks are less subject to changes

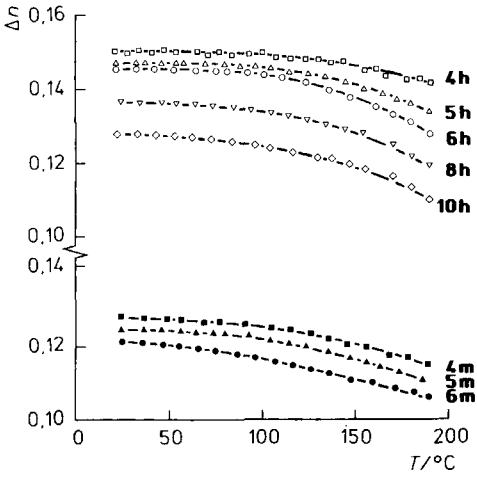

Fig. 11. Birefringence Δn as a function of the temperature of the polymer networks indicated. All polymer networks were polymerized at T_p/T_c = 0,93

in the ordering with temperature than low-molar-mass LCs or linear LC polymers. The changes in Δn are therefore small, especially at short spacer lengths. The slight loss of orientation at higher temperatures can be attributed to an increasing localized mobility of the aromatic rods above the glass transition temperature of the networks.

The decrease in optical retardation as a function of temperature is even smaller than that of Δn due to the compensating thermal expansion[6], an effect which is accounted for in the calculation of $\Delta n\,(T)$. It is interesting to note that the birefringence changes are perfectly reversible.

Conclusions

Variation of the spacer of LC diacrylate monomers from 4 to 11 methylene groups affects the mesomorphic properties. Increasing spacer length results in decreasing isotropic transition temperatures and stabilisation of the smectic phases. Macroscopic orientation of the nematic monomers on rubbed substrates yields a mono-domain-like texture with order parameters in accordance with those of conventional low-molar-mass LCs. At longer spacer lengths, the higher order parameters are prohibited due to the S_c phase, exhibiting director fluctuations.

The polymerization behaviour of the LC monomers is in accordance with that of isotropic diacrylates, i. e., high polymerization rates at low conversion and relatively low rates at high conversion where most monomeric units are attached to the network at at least one side of the molecule. The molecular ordering of the LC monomers suppresses termination by chain transfer, which is seen to occur during the polymerization of isotropic diacrylates above 90 °C. At higher temperatures, near the transition to isotropic, the polymerization rate of the LC diacrylates rapidly drops to the level of conventional isotropic diacrylates. The overall kinetics of polymerization is the same in the nematic and in the smectic phase.

The length of the flexible spacer has a small influence on the order parameter of the oriented networks. Spacer lengths smaller than six methylene units change the conformation of the aromatic core, which leads to smaller order parameters as measured by refractive indices and infrared dichroism, but it does not affect the order parameter of an added dye guest. The order parameter of the flexible spacer is in general somewhat lower than that of the aromatic core due to deviations from the all-*trans* configuration. In general, the order parameter is not subjected to large changes when the temperature is varied. When heated above the glass-transition temperature of the networks, the orientation decreases only marginally, as is concluded from birefringence measurements, and is retained upon cooling.

The polymer networks produced exhibit strongly anisotropic optical properties, such as a large birefringence and dichroism in the presence of a dye guest. The refractive indices can be varied by the spacer length, substituents and the polymerization temperature, yielding ordinary refractive indices between 1,52 and 1,55, and extraordinary refractive indices between 1,64 and 1,70.

Many people have contributed to the production of this paper. We especially wish to thank Mr. *J. Boven,* Dr. *W. ten Hoeve* and Dr. *J. Lub* for the syntheses of the various monomers, Mr. *A. R. J. Bouw* for his technical assistance with the infrared dichroic measurements, Dr. *A. G. J. Staring* for his help with the molecular modelling and Dr. *R. A. M. Hikmet* and Dr. *I. Heynderickx* for the discussions which lead to a better understanding of the subject. The work of two of the authors, D. J. B. and G. N. M., was supported by the *European Community* under *Brite Project P-1356-6-85.*

[1] D. J. Broer, J. Boven, G. N. Mol, G. Challa, *Makromol. Chem.* **190**, 2255 (1989)
[2] D. J. Broer, R. A. M. Hikmet, G. Challa, *Makromol. Chem.* **190**, 3201 (1989)
[3] H. Finkelmann, H. Ringsdorf, J. H. Wendorff, *Makromol. Chem.* **179**, 273 (1978)
[4] H. Finkelmann, M. Happ, M. Portugall, H. Ringsdorf, *Makromol. Chem.* **179**, 2541 (1978)
[5] R. A. M. Hikmet, D. J. Broer, *Polymer,* accepted for publication
[6] D. J. Broer, G. N. Mol, *Polym. Eng. Sci.,* accepted for publication
[7] D. J. Broer, H. Finkelmann, K. Kondo, *Makromol. Chem.* **189**, 185 (1988)
[8] D. J. Broer, G. N. Mol, G. Challa, *Makromol. Chem.* **190**, 19 (1989)
[9] J. F. Rabek, *"Experimental Methods in Polymer Chemistry"*, John Wiley and Sons, Chichester 1980, Ch. 35, p. 582
[10] M. F. Vuks, *Opt. Spectros. (USSR)* **20**, 361 (1966)
[11] S. Chandrasekhar, N. V. Madhusudana, *J. Phys. (Paris)* **30**, C4-24 (1969)
[12] I. Haller, H. A. Huggins, H. R. Lilienthal, T. R. McGuire, *J. Phys. Chem.* **22**, 950 (1973)
[13] R. G. Horn, *J. Phys. (Paris)* **39**, 105 (1978)
[14] F. Jones, T. J. Reeve, *J. Soc. Dyers Colour.* **95**, 352 (1979)
[15] H. Ringsdorf, H. W. Schmidt, G. Baur, R. Kiefer, F. Windscheid, *Liq. Cryst.* **1**, 319 (1986)
[16] W. Maier, G. Englert, *Z. Phys. Chem. (Frankfurt am Main)* **19**, 168 (1959)
[17] R. Kiefer, G. Baur, *Mol. Cryst. Liq. Cryst.* **174**, 101 (1989)
[18] R. Zbinden, *"Infrared Spectroscopy of High Polymers"*, Academic Press, New York 1964
[19] N. L. Allinger, Y. H. Yuh, *Quantum Chemistry Program Exchange* **13**, 395 (1981)
[20] N. L. Allinger, *Quantum Chemistry Program Exchange* **13**, 400 (1981)
[21] CHEMX, developed and distributed by Chemical Design Ltd., Oxford
[22] S. L. Arora, J. L. Fergason, T. R. Taylor, *J. Org. Chem.* **35**, 4055 (1970)
[23] M. J. S. Dewar, A. C. Griffin, *J. Am. Chem. Soc.* **97**, 6662 (1975)
[24] H. Kelker, R. Hatz, *"Handbook of Liquid Crystals"*, Verlag Chemie GmbH, Weinheim 1980, Ch. 8, p. 340
[25] J. M. Adams, S. E. Morsi, *Acta Crystallogr., Sect. B* **32**, 1345 (1976)
[26] R. A. M. Hikmet, D. J. Broer, *"Integration of Fundamental Polymer Science and Technology"*, ed. by L. A. Kleintjes, P. J. Lemstra, Elsevier Applied Science Publishers, London, in press
[27] H. Stenschke, *Solid State Commun.* **10**, 653 (1972)
[28] W. Maier, A. Saupe, *Z. Naturforsch., Teil A* **14**, 882 (1959); *ibid.* **15**, 287 (1960)
[29] A. Buka, W. H. de Jeu, *J. Phys. (Paris)* **43**, 361 (1982)
[30] J. Cognard, T. Hieu Phan, N. Basturk, *Mol. Cryst. Liq. Cryst.* **91**, 327 (1983)
[31] D. Bauman, *Mol. Cryst. Liq. Cryst.* **172**, 41 (1989); *ibid.* **174**, 1 (1989)
[32] D. J. Broer, I. Heynderickx, *Macromolecules* **23**, 2474 (1990)
[33] R. A. M. Hikmet, B. H. Zwerver, D. J. Broer, *Polymer,* submitted
[34] J. G. Kloosterboer, *Adv. Polym. Sci.* **84**, 1 (1988)
[35] D. J. Broer, G. N. Mol, G. Challa, *Polymer,* accepted for publication
[36] M. Portugall, H. Ringsdorf, R. Zentel, *Makromol. Chem.* **183**, 2311 (1982)
[37] L. J. Bellamy, *"The Infrared Spectra of Complex Molecules"*, Vol. 1, 3rd ed., Chapman and Hall, London 1975, p. 82